HHS Public Access

Author manuscript

Atherosclerosis. Author manuscript; available in PMC 2016 May 01.

Published in final edited form as:

Atherosclerosis. 2015 May ; 240(1): 163–173. doi:10.1016/j.atherosclerosis.2015.03.013.

GPR40/FFA1 and Neutral Sphingomyelinase Are Involved in Palmitate-Boosted Inflammatory Response of Microvascular Endothelial Cells to LPS

Zhongyang Lu[2], **Yanchun Li**[2], **Junfei Jin**[2,4], **Xiaoming Zhang**[2], **Yusuf A. Hannun**[3], and **Yan Huang**[1,2]

[1]Ralph H. Johnson Veterans Affairs Medical Center, Charleston, SC 29401

[2]Division of Endocrinology, Diabetes and Medical Genetics, Department of Medicine, Medical University of South Carolina, Charleston, SC 29425

[3]Stony Brook Cancer Center, Stony Brook University, Stony Brook, NY 11794

[4]Laboratory of Hepatobiliary and Pancreatic Surgery, Affiliated Hospital of Guilin Medical University, Guilin, 541001, Guangxi, People's Republic of China

Abstract

Objectives—Increased levels of both saturated fatty acids (SFAs) and lipopolysaccharide (LPS) are associated with type 2 diabetes. However, it remains largely unknown how SFAs interact with LPS to regulate inflammatory responses in microvascular endothelial cells (MIC ECs) that are critically involved in atherosclerosis as a diabetic complication. In this study, we compared the effects of LPS, palmitic acid (PA), the most abundant saturated fatty acid, or the combination of LPS and PA on interleukin (IL)-6 expression by MIC ECs and explored the underlying mechanisms.

Methods—Human cardiac MIC ECs were treated with LPS, PA and LPS plus PA and the regulatory pathways including receptors, signal transduction, transcription and post-transcription, and sphingolipid metabolism for IL-6 expression were investigated.

Results—G protein-coupled receptor (GPR)40 or free fatty acid receptor 1 (FFA1), but not toll-like receptor 4, was involved in PA-stimulated IL-6 expression. PA not only stimulated IL-6 expression by itself, but also remarkably enhanced LPS-stimulated IL-6 expression via a cooperative stimulation on mitogen-activated protein kinase and nuclear factor kappa B signaling pathways, and both transcriptional and post-transcriptional activation. Furthermore, PA induced a

Corresponding author: Yan Huang, M.D., Ph.D., Ralph H. Johnson Veterans Affairs Medical Center, and Division of Endocrinology, Diabetes and Medical Genetics, Department of Medicine, Medical University of South Carolina, 114 Doughty St. Charleston, SC29425, Tel: (843) 789-6824; Fax: (843) 876-5133; huangyan@musc.edu.

Conflict of interest

None.

robust neutral sphingomyelinase (nSMase)-mediated sphingomyelin hydrolysis that was involved in PA-augmented IL-6 upregulation.

Conclusion—PA boosted inflammatory response of microvascular endothelial cells to LPS via GPR40 and nSMase.

Keywords

Atherosclerosis; Palmitic acid; LPS; Sphingolipid; Endothelium

1. Introduction

It is known that microvascular system plays an important role in the progression of atherosclerosis as the system frequently develops inside atherosclerotic plaques to supply oxygen and nutrients for lesion development [1]. Furthermore, studies have indicated that microvascular system in advanced plaques contribute to intraplaque hemorrhage and plaque rupture [1–3]. Microvascular endothelial cells (MIC ECs) constituting the microvascular system proliferate mainly from the vasa vasorum and penetrate into the intima [1].

To understand the mechanisms involved in MIC EC-associated atherosclerosis, we have shown that MIC ECs exhibit a robust inflammatory response to lipopolysaccharide (LPS), a potent ligand to activate toll-like receptor (TLR)4[4], and interact with mononuclear cells through secreted interleukin (IL)-6, leading to a remarkable increase in matrix metalloproteinase production [5]. LPS is present in the circulation at low concentrations and studies have shown that the serum LPS activity is correlated with several risk factors of atherosclerosis such as chronic inflammation, dyslipidemia, obesity, and diabetes [6, 7].

In addition to LPS, patients with obesity, metabolic syndrome or diabetes also have increased serum level of saturated fatty acids (SFA) [8]. It has been shown that palmitic acid (PA), the most abundant SFA, aggravates neointima formation [9]. Given that the serum levels of both SFA and LPS are elevated in patients with obesity, metabolic syndrome and type 2 diabetes [10], and MIC ECs are the first line of cells to directly interact with circulating SFAs and LPS, it is important to elucidate how SFAs and LPS interact to stimulate inflammatory response of MIC ECs.

In this study, we employed human cardiac MIC ECs and focused on the regulation by LPS and/or PA of the expression of IL-6, a key proinflammatory cytokine involved in atherosclerosis [11]. We found that PA not only stimulated IL-6 expression by itself, but also augmented the stimulation of LPS on IL-6 expression. We also found that G protein-coupled receptor (GPR)40, also called free fatty acid receptor 1 (FFA1), and neutral sphingomyelinase (nSMase) were involved in the PA-augmented IL-6 expression.

2. Materials and methods

2.1. Cell culture

Human cardiac MIC ECs (Lonza, Allendale, NJ) were grown in EGM™-2 media containing 5% fetal bovine serum, 0.04% hydrocortisone, 0.4% basic fibroblast growth factor, 0.1% vascular endothelial growth factor, 0.1% insulin-like growth factor-1 and 0.1% 0.5 epithelial

growth factor. The ECs between passage 4 and 8 were used for the experiments. For all experiments, cultures of MIC ECs were 100% confluent before the treatments. PA, oleic acid (OA) and docosahexaenoic acid (DHA) (Sigma, St. Louis, MO) was dissolved in 0.1 N NaOH and 70% ethanol at 70 °C to make 50 mM concentration. The solution was kept at 55 °C for 10 min and then brought to room temperature. To make PA conjugated with BSA, the 50 mM PA solution was added dropwise into 5% BSA with low endotoxin and without FA (Sigma) to make a final stock of 5 mM PA (final PA/BSA ratio was 2.3:1). The solution was kept at 55°C for 10 min, mixed, and brought to room temperature. Unless otherwise specified, PA without BSA was used in the experiments.

2.2. Enzyme-linked immunosorbent assay (ELISA)

IL-6 in medium was quantified using sandwich ELISA kits according to the protocol provided by the manufacturer (Biolegend, San Diego, CA).

2.3. Real-time polymerase chain reaction (PCR)

Total RNA was isolated from cells using RNeasy minikit (Qiagen, Santa Clarita, CA). First-strand complementary DNA (cDNA) was synthesized with the iScript™ cDNA synthesis kit (Bio-Rad Laboratories, Hercules, CA) using 20 μl of reaction mixture containing 0.5 μg of total RNA, 4 μl of 5x iScript reaction mixture, and 1 μl of iScript reverse transcriptase. The complete reaction was cycled for 5 minutes at 25 °C, 30 minutes at 42 °C and 5 minutes at 85°C using a PTC-200 DNA Engine (MJ Research, Waltham, MA). The reverse transcription reaction mixture was then diluted 1:10 with nuclease-free water and used for PCR amplification in the presence of the primers. The Beacon designer software (PREMIER Biosoft International, Palo Alto, CA) was used for primer designing (Human *IL6*: Forward sequence, TGGAGTCACAGAAGGAGTGGCTAAG; Reverse sequence, TCTGACCACAGTGAGGAATGTCCAC. Human *gpr40*: Forward sequence, TCAGCCTCTCTCTCCTGCTC; Reverse sequence, CGCACACACTGTCTTCAGGC. Human nSMase2: Forward sequence, AGGACTGGCTGGCTGATTTC; Reverse sequence, TGTCGTCAGAGGAGCAGTTAT). Primers were synthesized by Integrated DNA Technologies, Inc. (Coralville, IA). Real-time PCR was performed in duplicate using 25 μl of reaction mixture containing 1.0 μl of RT mixture, 0.2 μM of both primers, and 12.5 μl of iQ™ SYBR Green Supermix (Bio-Rad Laboratories). Real-time PCR was run in the iCycler™ real-time detection system (Bio-Rad Laboratories) with a two-step method. The hot-start enzyme was activated (95°C for 3 min) and cDNA was then amplified for 40 cycles consisting of denaturation at 95°C for 10 sec and annealing/extension at 60°C for 45 sec. A melt-curve assay was then performed (55°C for 1 min and then temperature was increased by 0.5°C every 10 sec) to detect the formation of primer-derived trimmers and dimmers. Glyceraldehyde 3-phosphate dehydrogenase (*gapdh*) was used as a control (Forward primer sequence, GAATTTGGCTACAGCAACAGGGTG; Reverse primer sequence, TCTCTTCCTCTTGTGCTCTTGCTG). Data were analyzed with the iCycler iQ™ software. The average starting quantity (SQ) of fluorescence units was used for analysis. Quantification was calculated using the SQ of targeted cDNA relative to that of GAPDH cDNA in the same sample.

2.4. PCR arrays

First-strand cDNA was synthesized from RNA using RT^2 First Strand Kit (Qiagen). Human TLR signaling pathway-focused PCR Array (Catalog # PAHS-018Z, Qiagen) was performed using 2X SuperArray RT^2 qPCR master mix and the first strand cDNA by following the instruction from the manufacturer.

2.5. IL-6 mRNA stability analysis

Human cardiac MIC ECs were treated with 5 ng/ml of LPS, 100 μM of PA or LPS plus PA for 4 hours, followed by addition of 5 μg/ml of actinomycin D (Sigma-Aldrich Corporate, St. Louis, MO). The incubation was continued for 2 and 4 hours after the addition of actinomycin D. The cells were then harvested and cellular IL-6 mRNA was quantified using real-time PCR as described above.

2.6. Immunoblotting

Cytoplasmic protein of each sample (50 μg) was electrophoresed in a 10% polyacrylamide gel. After transferring proteins to a PVDF membrane, total and phosphorylated mitogen-activated protein kinase (MAPK) including extracellular signal-regulated kinase (ERK), Jun N-terminal kinase (JNK) and p38 MAPK were immunoblotted with anti-total and anti-phosphorylated MAPK primary antibodies (Cell Signaling Technology, Danvers, MA), respectively, and horseradish peroxidase (HRP)-conjugated secondary antibody. After washing, the kinases was detected by incubating the membrane with chemiluminescence reagent (NEN Life Science Products) for 1 min and exposing it to x-ray film for 15–60 seconds. The X-ray films were scanned using an Epson scanner (Perfection 1200U) and the density of bands on the images was quantified using NIH Image version 1.63. The results were presented as the ratios of phosphorylated kinase vs. total kinase. Immunoblotting of GPR40 was also performed using anti-GPR40 antibody (Santa Cruz Biotechnology, Inc. Santa Cruz, CA).

2.7. Transfection and luciferase activity assay

Human cardiac MIC ECs were transfected with 1 μg of nuclear factor kappa B (NFκB) Cignal Reporter (Qiagen) using FuGENE 6 (Promega, Madison, WI) as transfection reagent for 8 h. The renilla luciferase constructs were used as control. The cells were then treated with fresh medium containing 5 ng/ml LPS, 100 μM PA or LPS plus PA for 24 h. After the treatment, the cells were rinsed with cold PBS and lysed with the buffer from Dual-Luciferase Reporter Assay System (Promega). Both firefly and renilla luciferase levels were measured in a luminometer using the dual-luciferase reporter assay reagents (Promega) according to the instruction from the manufacturer. The firefly luciferase levels were normalized to the renilla luciferase levels.

2.8. Lipidomics

Human cardiac MIC ECs were collected, fortified with internal standards, extracted with ethyl acetate/isopropyl alcohol/water (60:30:10, v/v/v), evaporated to dryness, and reconstituted in 100 μl of methanol. Simultaneous ESI/MS/MS analyses of sphingoid bases, sphingoid base 1-phosphates, CERs, and SM were performed on a Thermo Finnigan TSQ

7000 triple quadrupole mass spectrometer operating in a multiple reaction monitoring positive ionization mode. The phosphate contents of the lipid extracts were used to normalize the MS measurements of sphingolipids. The phosphate contents of the lipid extracts were measured with a standard curve analysis and a colorimetric assay of ashed phosphate [12].

2.9. Treatment of cells with inhibitors of MAPK and NFκB pathways, and sphingolipid metabolism

Human cardiac MIC ECs were treated with 5 ng/ml LPS, 100 μM PA or LPS plus PA in the absence or presence of 5 or 10 μM of PD98059, SP600125, SB203580, 1 or 5 μM of Bay117085 (Calbiochem/EMD Biosciences, Inc., San Diego, CA) for 24 h. After the treatment, IL-6 in medium was quantified using ELISA. For experiments on sphingolipid pathway, human cardiac MIC ECs were treated with 5 ng/ml LPS, 100 μM PA or LPS plus PA in the absence or presence of imipramine hydrochloride (Sigma-Aldrich Corporate), GW4869 (Sigma-Aldrich Corporate), myriocin (Cayman Chemical, Ann Arbor, MI), or fumonisin B1 (Cayman Chemical) for 24 hours. After the treatment, IL-6 in culture medium was quantified using ELISA.

2.10. RNA interference

Human cardiac MIC ECs were transiently transfected with 10 nM of GPR40 siRNA, nSMase siRNA or scrambled siRNA control (Santa Cruz Biotechnology, Inc.) using Lipofectamine™ RNAiMAX (Life Technologies, Grand Island, NY) by following the manufacturer's instructions. Twenty-four hours later, transfected cells were treated with or without 5 ng/ml LPS, 100 μM PA or LPS plus PA for 24 h.

2.11. Statistic analysis

The experiments were performed 3 times and the data were presented as mean ± SD. One-way ANOVA was performed to determine the statistical significance of cytokine expression among different experimental groups. A value of $P < 0.05$ was considered significant.

3. Results

3.1. PA not only stimulates IL-6 expression, but also augments the effect of LPS

We first determined the effect of PA, LPS or PA plus LPS on IL-6 secretion in cardiac MIC ECs. Results showed that while LPS stimulated IL-6 secretion in a concentration-dependent manner, PA further augmented the stimulatory effect of LPS on IL-6 secretion (Fig. 1A). Since we used BSA-free PA in this study, we compared the effects of BSA-free PA and PA conjugated with low endotoxin BSA on LPS-stimulated IL-6 secretion. Results showed that while BSA-free PA and BSA-conjugated PA increased IL-6 secretion similarly, they also exerted a similar effect on enhancement of LPS-stimulated IL-6 secretion (Fig. 1B). Furthermore, to show the effects of unsaturated fatty acids on LPS signaling, we treated cardiac MC ECs with oleic acid (OA) or docosahexaenoic acid (DHA) in the absence or presence of LPS. Results showed that OA and DHA not only inhibited IL-6 secretion by themselves, but also attenuated the effect of LPS on IL-6 secretion (Fig. 1C). Additionally,

OA and DHA also inhibited PA-stimulated IL-6 secretion (Fig. 1C). These findings clearly reveal the specificity of PA in the enhancement of LPS-triggered signaling.

To characterize the effect of LPS, PA or LPS plus PA on IL-6 expression, we performed time course studies on IL-6 mRNA expression and protein secretion. As shown in Fig. 1D, the kinetics of IL-6 mRNA expression stimulated by PA is strikingly different from that by LPS. LPS stimulated a quick but brief increase in IL-6 mRNA with a peak at 4 h while PA induced a delayed but prolonged IL-6 mRNA expression. Further, the kinetics of IL-6 mRNA expression stimulated by the combination of PA and LPS was also remarkably different from that stimulated by LPS alone. The combination of LPS and PA not only prevented the sharp decrease of IL-6 mRNA observed in cells treated with LPS alone at 8 h, but also stimulated a high and prolonged IL-6 mRNA expression (Fig. 1D).

Consistent with the kinetics of mRNA expression, the quantification of IL-6 protein in culture medium showed that LPS alone induced a quick IL-6 secretion at 8 h while PA stimulated a delayed but persistent increase in IL-6 protein secretion (Fig. 1E). Moreover, the combination of LPS and PA led to a liner and remarkable increase in IL-6 secretion. Thus, these data showed that LPS and PA exerted a synergistic effect on IL-6 expression.

To further define the effects of LPS and PA on the cellular inflammatory response, we performed gene expression analysis using a PCR array. As shown in Table 1, either LPS (4-h stimulation) or PA (36-h stimulation) had similar stimulation on several inflammatory cytokines such as colony stimulating factors (CSFs), IL-1, IL-6, IL-8, and TNFα. The genes stimulated by both LPS and PA were accounted for 60% of all genes upregulated by 2-fold or more by LPS or PA. Interestingly, LPS and PA also stimulated different genes. For example, LPS stimulated chemokine C-C motif ligand 2 (CCL2 or MCP-1) and chemokine C-X-C motif ligand 10 (CXCL10) while PA stimulated c-Fos, heat-shock protein 1A (HSPA1A) and IFNγ, suggesting that LPS and PA do not share a regulatory pathway for gene expression. Furthermore, the PCR array analysis showed that the combination of LPS and PA (36-h stimulation) led to an increased expression of many important genes such as CSF2, CSF3, FOS, IL-1β and PTGS2 as compared to LPS or PA alone (Table 2), revealing a potential synergy between LPS and PA on vascular inflammation.

3.2. GPR40, but not TLR4, mediates PA-stimulated IL-6 expression

We next determined if TLR4 is involved in PA-stimulated IL-6 upregulation since it was reported previously that PA-stimulated gene expression in ECs was mediated by TLR4[13]. Results showed that the anti-TLR4 antibodies effectively inhibited LPS-stimulated IL-6 in a concentration-dependent manner (Fig. 2A), but failed to block the stimulatory effect of PA (Fig. 2B), indicating that TLR4 does not mediate PA-stimulated IL-6 expression. Since the recent studies showed that GPR40/FFA1 was expressed by pancreatic beta cells and mediated the actions of PA in inducing beta cell apoptosis [14, 15] and GPR40/FFA1 is known to be expressed by MIC ECs [16, 17], we determined if GPR40 plays a role in PA-stimulated IL-6 expression in human cardiac MIC ECs. Using GPR40 selective antagonist GW1100[18], our study showed that antagonizing GPR40 effectively inhibited PA-stimulated IL-6 secretion (Fig. 2C). Surprisingly, results showed that GW1100 also inhibited LPS-stimulated IL-6 secretion, suggesting that the binding of GPR40 by GW1100 may activate signaling

pathways that interfere LPS-triggered TLR4 signaling. To corroborate the above findings, we transfected cells with GPR40 siRNA to knock down GPR40 mRNA level (Fig. 2D). Results showed that the knockdown of GPR40 mRNA expression by siRNA markedly reduced PA-stimulated IL-6 expression (Fig. 2E). We further determined if GPR40 is involved in OA-inhibited LPS signaling and results showed that GPR40 antagonist GW1100 did not neutralize the inhibitory effect of OA on LPS-stimulated IL-6 by LPS (Fig. 2F), suggesting that GPR40 does not mediate the effect of OA. Taken together, these data indicate that GPR40, but not TLR4, is involved in PA-stimulated IL-6 expression in human cardiac MIC ECs.

Since it is known that the MAPK and NFκB signaling pathways are involved in IL-6 expression [19, 20], we determined if PA activates MAPK and NFκB pathways in human cardiac MIC ECs. The results showed that PA stimulated the phosphorylation of ERK (Fig. 3A), JNK (Fig. 3B) and p38 MAPK (Fig. 3C) in a time-dependent manner and the kinetics of the phosphorylation stimulated by PA is similar to that stimulated by LPS. Interestingly, quantification of phosphorylated EKR, JNK and p38 MAPK showed that LPS and PA cooperatively stimulated the phosphorylation of ERK (Fig. 3A) and JNK (Fig. 3B). For NFκB pathway, we used a luciferase reporter system to determine the effect of LPS, PA or LPS plus PA on NFκB activity. Results showed that while either LPS or PA increased NFκB activity, LPS plus PA further augmented it (Fig. 3D). Furthermore, we determined if MAPK and NFκB pathways are required for PA-stimulated IL-6 expression using pharmacological inhibitors. Results showed that the ERK pathway inhibitor PD98059, JNK pathway inhibitor SP600126, p38 MAPK pathway inhibitor SB203580, and NFκB pathway inhibitor Bay11-7082 inhibited the stimulatory effect of LPS, PA or LPS plus PA on IL-6 secretion in a dose-dependent manner (Fig. 3E and F).

3.3. PA enhances LPS-stimulated IL-6 expression through both transcriptional and post-transcriptional regulations

In this study, we determined if the enhancement of LPS-stimulated IL-6 expression by PA was achieved via transcriptional and/or post-transcriptional regulation. Results showed that when actinomycin D (Act D), a potent transcription inhibitor [21], was added to cells before the treatment with LPS plus PA, it inhibited IL-6 expression stimulated with LPS plus PA by 98% (Fig. 4A), indicating that transcriptional activation is responsible for IL-6 upregulation by LPS plus PA. This result also indicates that Act D at 5 μg/ml is capable of virtually abolishing IL-6 transcription, which is important for the next study in which complete inhibition of IL-6 transcription is required to evaluate the effect of PA on post-transcriptional regulation of IL-6.

In the study to determine if PA also enhances LPS effect through post-transcriptional regulation, we first stimulated cells with LPS or LPS plus PA for 4 h in the absence of Act D to induce IL-6 expression. The reason to select 4 h as the stimulation period is that Fig. 1B showed that stimulation with LPS or LPS plus PA for 4 h led to a marked increase in IL-6 mRNA expression. After 4-h stimulation, Act D (5 μg/ml) was added to part of the wells and the stimulation with LPS or LPS plus PA was continued for the next 4 h. The IL-6 mRNA levels before addition of Act D (0 h), 2 h and 4 h were quantified and IL-6 mRNA level at 0

h before the addition of Act D was considered as 100%. Results (Fig. 4B) showed that, without Act D, IL-6 expression by cells treated with LPS was reduced by 75% at 4 h, which is in agreement with the results shown in Fig. 1B. With Act D, IL-6 expression by cells treated with LPS was reduced by 62% at 4 h, suggesting that newly synthesized protein (s) is involved in IL-6 mRNA degradation. In cells treated with LPS plus PA in the absence of Act D, IL-6 expression was increased at 2 h and then slightly decreased, which is consistent with the results shown in Fig. 1B. However, when cells were treated with LPS plus PA in the presence of Act D, IL-6 expression was reduced by 43% at 4 h. These findings indicate that the upregulation of IL-6 expression at 4 h by LPS plus PA is largely controlled at the transcriptional level since Act D reverses IL-6 mRNA expression from upregulation to downregulation. Importantly, with Act D, IL-6 mRNA degradation at 4 h in cells treated with LPS alone was more than that in cells treated with LPS plus PA (62% vs 43%) (Fig. 4B), suggesting that addition of PA to LPS increased not only IL-6 transcription, but also IL-6 mRNA stability.

3.4. PA induces a robust sphingomyelin (SM) hydrolysis that is involved in the IL-6 upregulation

Since it has been reported that ceramide (CER), a bioactive sphingolipid, is involved in LPS-stimulated expression of proinflammatory genes [22, 23] and SM hydrolysis plays a major role in CER production (Fig. 5A), we determined if SM hydrolysis is involved in the augmentation of LPS-stimulated IL-6 expression by PA in human cardiac MIC ECs. Strikingly, our lipidomic study showed that PA robustly reduced cellular SM content by 53% (12.25 vs 26.42 pmol/nmol Pi), but LPS only reduced SM by 6% (24.93 vs 26.42 pmol/nmol Pi) (Fig. 5B). The combination of LPS and PA did not further reduce SM hydrolysis as compared to PA alone. We then determined if SM hydrolysis by is involved in PA-increased IL-6 expression by inhibiting either acid sphingomyelinase (aSMase) or neutral sphingomyelinase (nSMase). Both aSMase and nSMase are responsible for hydrolyzing SM (Fig. 5A). Results showed that imipramine, a pharmacological inhibitor of aSMase, had no effect on IL-6 secretion induced by LPS, PA or LPS plus PA (Fig. 5C), but GW4869, an inhibitor of nSMase, inhibited it significantly (Fig. 5D). In a parallel experiment, our lipidomics data showed that PA hydrolyzed 42% of SM in the absence of GW4869, but hydrolyzed 17% of SM in the presence of GW4869 (Table 3). Furthermore, since nSMase 2 has been shown to play a key role in the inflammatory response in ECs [24], we knocked down nSMase 2 mRNA expression using siRNA transfection to assess the role of nSMase 2 in IL-6 upregulation. Results showed that knockdown of nSMase 2 mRNA expression (Fig. 5E) potently inhibited the stimulation of IL-6 secretion by LPS, PA or PA plus LPS (Fig. 5F).

3.5. De novo synthesis of CER is also involved in IL-6 upregulaton by LPS or LPS plus PA

In addition to SM hydrolysis, the *de novo* synthesis of CER also contributes to the cellular CER level (Fig. 6A). In this study, we first determined the regulation of cellular level of CER by LPS, PA or LPS plus PA. Our lipidomic study showed that PA increased CER and the combination of LPS and PA further increased it (Fig. 6B). We then used the inhibitors for the *de novo* synthesis of CER to determine if the *de novo* synthesis of CER is involved in IL-6 upregulation. Results showed that myriocin, an inhibitor of serine palmitoytransferase

(SPT) [25], or fumonisin B1, an inhibitor of CER synthase [26], inhibited LPS-stimulated IL-6 secretion by 35% and 30%, respectively (Fig. 6C and 6D). Results also showed that myriocin and fumonisin B1 inhibited IL-6 secretion stimulated by LPS plus PA by 30%. In contrast, myriocin and fumonisin B1 failed to inhibit PA-stimulated IL-6 secretion (Fig. 6C and 6D), suggesting that the *de novo* synthesis of CER is involved in IL-6 upregulation stimulated by LPS and LPS plus PA, but not PA alone. Consistently, our lipidomics data (Table 4) showed that myriocin reduced CER production in cells treated with LPS or LPS plus PA, but had no effect on PA-increased CER production, suggesting that PA-increased CER production is largely derived from SM hydrolysis.

4. Discussion

PA has been considered as an endogenous ligand for TLR4, but this notion was challenged by the reports that BSA used for PA conjugation has LPS contamination that is likely the cause of TLR4 ligation [27, 28]. In the current study, we used BSA-free PA as reported previously to preclude LPS contamination [29]. In the study of Schwartz et al., BSA-free PA was considered to complex with the BSA already present in the 10% fetal bovine serum in the culture medium [29]. This notion, however, has not been confirmed. To determine if BSA-free PA has similar stimulation as PA conjugated with BSA, we compared the effects of BSA-free PA and PA conjugated with low endotoxin BSA on IL-6 upregulation by LPS. Result showed that BSA-free PA and PA conjugated with low endotoxin BSA exerted a similar effect on the enhancement of LPS-stimulated IL-6 secretion (Fig. 1B).

Our findings demonstrate that GPR40, but not TLR4, plays an important role in the upregulation of IL-6 by PA in human cardiac MIC ECs. GPR40, a G protein-coupled receptor also called FFA1, is expressed abundantly in the pancreatic β-cells and serves as receptor for long-chain FFAs [30]. It has been shown that activation of GPR40 by long-chain FFAs leads to an enhanced β-cell response to glucose in the secretion of insulin [31]. Thus, GPR40 activation has been proposed as a therapeutic strategy to increase insulin secretion in treatment of diabetes. However, recent studies have shown that GPR40 mediates the effect of PA on beta-cell apoptosis [14, 15]. These studies indicate that although different free fatty acids and synthetic agonists are capable of engaging GPR40, they can elicit different GPR40-mediated signaling cascades, leading to diverse cellular functions. In supporting this notion, our current study demonstrated for the first time that GPR40 in human cardiac MIC ECs mediated PA-stimulated proinflammatory cytokine expression.

It is noteworthy that the stimulatory effect of PA on IL-6 expression in cardiac MIC ECs is cell type specific since PA failed to stimulate IL-6 expression in macrophages although it enhances the effect of LPS on IL-6 expression [32]. Furthermore, our time-course study as shown in Fig. 1B suggested that the regulatory pathways involved in the stimulation of IL-6 expression by PA and LPS are strikingly different. First, there was a 12 h-delay in IL-6 mRNA expression in response to PA, which contrasts the rapid rise of IL-6 expression with a peak at 4 h in response to LPS. Second, PA-stimulated IL-6 expression was gradually increased after 12 h delay and plateaued at the high level after 36 h, which is sharply different from the rapidly declined IL-6 expression after 4 h in response to LPS. It appears that LPS initiates an “acute” action, but PA exerts a “chronic” effect on IL-6 expression.

It is intriguing to find that the combination of PA and LPS dramatically increased IL-6 mRNA expression in both extent and duration (Fig. 1B). Although the underlying mechanisms have not been completely understood, our study has shed lights into the interaction between LPS and PA. First, LPS and PA had an additive effect on ERK, JNK and NFκB signaling activation that is known to mediate IL-6 upregulation. Second, our data showed that PA enhanced LPS-stimulated IL-6 expression via both transcriptional and post-transcriptional regulations. Since IL-6 mRNA is unstable and readily degraded by RNase [33], this finding suggests that PA inhibits RNase-mediated IL-6 mRNA degradation in addition to its stimulation on IL-6 transcription.

Active sphingolipids play an important role in regulating expression of pro-inflammatory genes [32, 34]. Therefore, we sought to elucidate the interactions between LPS and PA on sphingolipid metabolism in human cardiac MIC ECs and determine if sphingolipids are involved in IL-6 upregulation by LPS and PA. Surprisingly, results showed that PA stimulated a robust SM hydrolysis by reducing 53% of the cellular SM. Further investigations revealed that nSMase, but not aSMase, was responsible for PA-stimulated SM hydrolysis. The involvement of nSMase in SM hydrolysis in cardiac MIC ECs is interesting since our recent study showed that aSMase contributed to SM hydrolysis in response to PA in macrophages [32]. Previously, studies have shown that different inflammatory mediators regulate gene expression via either nSMase- or aSMase-mediated SM hydrolysis in vascular ECs. For example, TNFα stimulated endothelial nitric oxide synthase (eNOS) via nSMase-mediated SM hydrolysis [35], but platelet-activating factor reduced eNOS production via aSMase [36]. Here, we showed for the first time that same stimulus like PA activated different SMase in different types of cells to promote inflammatory response.

In addition to the effect of PA on SM hydrolysis that generates CER, it is known that PA also increases cellular content of palmitoyl-CoA, a substrate for the *de novo* synthesis of CER [37, 38]. Interestingly, our present study showed that while myriocin, an inhibitor of SPT that is the initial and rate-limiting enzyme for the *de novo* CER synthesis, reduced CER in cells treated with LPS and LPS plus PA, it failed to decrease PA-stimulated CER (Table 4), suggesting that the CER increase in response to PA was mainly derived from SM hydrolysis. This data are consistent with our observation that myriocin had no effect on PA-stimulated IL-6 secretion (Fig. 6C).

In conclusion, our study demonstrated that PA and LPS exerted a cooperative stimulation via GPR40 and TLR4, respectively, on MAPK and NFκB signaling pathways, leading to IL-6 upregulation. Moreover, our study also demonstrated that PA stimulated a robust nSMase-mediated SM hydrolysis and subsequent CER production, which contributed to PA-stimulated IL-6 upregulation.

Acknowledgments

This work was supported by the Biomedical Laboratory Research and Development Program of the Department of Veterans Affairs and NIH grant DE016353 (to Y.H.) and grants GM43825 and CA97132 (to Y.A.H.). The work on sphingolipid analysis was supported in part by the Lipidomics Shared Resource, Hollings Cancer Center, Medical University of South Carolina (P30 CA138313), the Lipidomics Core in the SC Lipidomics and Pathobiology COBRE (P20 RR017677) and the National Center for Research Resources and the Office of the Director of the National Institutes of Health through Grant Number C06 RR018823.

References

1. Moulton KS. Angiogenesis in atherosclerosis: gathering evidence beyond speculation. Curr Opin Lipidol. 2006; 17:548–555. [PubMed: 16960504]
2. Moreno PR, Purushothaman KR, Zias E, et al. Neovascularization in human atherosclerosis. Curr Mol Med. 2006; 6:457–477. [PubMed: 16918368]
3. Ribatti D, Levi-Schaffer F, Kovanen PT. Inflammatory angiogenesis in atherogenesis--a double-edged sword. Ann Med. 2008; 40:606–621. [PubMed: 18608127]
4. Cani PD, Osto M, Geurts L, et al. Involvement of gut microbiota in the development of low-grade inflammation and type 2 diabetes associated with obesity. Gut Microbes. 2012; 3:279–288. [PubMed: 22572877]
5. Lu Z, Li Y, Jin J, et al. Toll-like receptor 4 activation in microvascular endothelial cells triggers a robust inflammatory response and cross talk with mononuclear cells via interleukin-6. Arterioscler Thromb Vasc Biol. 2012; 32:1696–1706. [PubMed: 22596222]
6. Lassenius MI, Pietilainen KH, Kaartinen K, et al. Bacterial endotoxin activity in human serum is associated with dyslipidemia, insulin resistance, obesity, and chronic inflammation. Diabetes Care. 2011; 34:1809–1815. [PubMed: 21636801]
7. Piya MK, McTernan PG, Kumar S. Adipokine inflammation and insulin resistance: the role of glucose, lipids and endotoxin. J Endocrinol. 2013; 216:T1–T15. [PubMed: 23160966]
8. Cascio G, Schiera G, Di Liegro I. Dietary fatty acids in metabolic syndrome, diabetes and cardiovascular diseases. Curr Diabetes Rev. 2012; 8:2–17. [PubMed: 22414056]
9. Shen H, Eguchi K, Kono N, et al. Saturated fatty acid palmitate aggravates neointima formation by promoting smooth muscle phenotypic modulation. Arterioscler Thromb Vasc Biol. 2013; 33:2596–2607. [PubMed: 23968977]
10. Colwell GA. Inflammation and diabetic vascular complications. Diabetes Care. 1999; 22:1927–1928. [PubMed: 10587819]
11. Kishimoto T. Interleukin-6: discovery of a pleiotropic cytokine. Arthritis Res Ther. 2006; 8 (Suppl 2):S2. [PubMed: 16899106]
12. Van Veldhoven PP, Bell RM. Effect of harvesting methods, growth conditions and growth phase on diacylglycerol levels in cultured human adherent cells. Biochim Biophys Acta. 1988; 959:185–196. [PubMed: 3349097]
13. Maloney E, Sweet IR, Hockenbery DM, et al. Activation of NF-kappaB by palmitate in endothelial cells: a key role for NADPH oxidase-derived superoxide in response to TLR4 activation. Arterioscler Thromb Vasc Biol. 2009; 29:1370–1375. [PubMed: 19542021]
14. Natalicchio A, Labarbuta R, Tortosa F, et al. Exendin-4 protects pancreatic beta cells from palmitate-induced apoptosis by interfering with GPR40 and the MKK4/7 stress kinase signalling pathway. Diabetologia. 2013; 56:2456–2466. [PubMed: 23995397]
15. Wu J, Sun P, Zhang X, et al. Inhibition of GPR40 protects MIN6 beta cells from palmitate-induced ER stress and apoptosis. J Cell Biochem. 2012; 113:1152–1158. [PubMed: 22275065]
16. Ma D, Lu L, Boneva NB, et al. Expression of free fatty acid receptor GPR40 in the neurogenic niche of adult monkey hippocampus. Hippocampus. 2008; 18:326–333. [PubMed: 18064707]
17. Honore JC, Kooli A, Hamel D, et al. Fatty acid receptor Gpr40 mediates neuromicrovascular degeneration induced by transarachidonic acids in rodents. Arterioscler Thromb Vasc Biol. 2013; 33:954–961. [PubMed: 23520164]
18. Briscoe CP, Peat AJ, McKeown SC, et al. Pharmacological regulation of insulin secretion in MIN6 cells through the fatty acid receptor GPR40: identification of agonist and antagonist small molecules. Br J Pharmacol. 2006; 148:619–628. [PubMed: 16702987]
19. Ji G, Zhang Y, Yang Q, et al. Genistein suppresses LPS-induced inflammatory response through inhibiting NF-kappaB following AMP kinase activation in RAW 264. 7 macrophages. PLoS One. 2012; 7:e53101. [PubMed: 23300870]
20. Guimaraes MR, Leite FR, Spolidorio LC, et al. Curcumin abrogates LPS-induced pro-inflammatory cytokines in RAW 264.7 macrophages. Evidence for novel mechanisms involving SOCS-1, -3 and p38 MAPK. Arch Oral Biol. 2013; 58:1309–1317. [PubMed: 24011306]

21. Sobell HM. Actinomycin and DNA transcription. Proc Natl Acad Sci U S A. 1985; 82:5328–5331. [PubMed: 2410919]
22. Haimovitz-Friedman A, Cordon-Cardo C, Bayoumy S, et al. Lipopolysaccharide induces disseminated endothelial apoptosis requiring ceramide generation. J Exp Med. 1997; 186:1831–1841. [PubMed: 9382882]
23. MacKichan ML, DeFranco AL. Role of ceramide in lipopolysaccharide (LPS)-induced signaling. LPS increases ceramide rather than acting as a structural homolog. J Biol Chem. 1999; 274:1767–1775. [PubMed: 9880559]
24. De Palma C, Meacci E, Perrotta C, et al. Endothelial nitric oxide synthase activation by tumor necrosis factor alpha through neutral sphingomyelinase 2, sphingosine kinase 1, and sphingosine 1 phosphate receptors: a novel pathway relevant to the pathophysiology of endothelium. Arterioscler Thromb Vasc Biol. 2006; 26:99–105. [PubMed: 16269668]
25. Cowart LA, Hannun YA. Selective substrate supply in the regulation of yeast *de novo* sphingolipid synthesis. J Biol Chem. 2007; 282:12330–12340. [PubMed: 17322298]
26. Mullen TD, Jenkins RW, Clarke CJ, et al. Ceramide synthase-dependent ceramide generation and programmed cell death: involvement of salvage pathway in regulating postmitochondrial events. J Biol Chem. 2011; 286:15929–15942. [PubMed: 21388949]
27. Erridge C, Samani NJ. Saturated fatty acids do not directly stimulate Toll-like receptor signaling. Arterioscler Thromb Vasc Biol. 2009; 29:1944–1949. [PubMed: 19661481]
28. Erridge C. Endogenous ligands of TLR2 and TLR4: agonists or assistants? J Leukoc Biol. 2010; 87:989–999. [PubMed: 20179153]
29. Schwartz EA, Zhang WY, Karnik SK, et al. Nutrient modification of the innate immune response: a novel mechanism by which saturated fatty acids greatly amplify monocyte inflammation. Arterioscler Thromb Vasc Biol. 2010; 30:802–808. [PubMed: 20110572]
30. Feng XT, Leng J, Xie Z, et al. GPR40: a therapeutic target for mediating insulin secretion (review). Int J Mol Med. 2012; 30:1261–1266. [PubMed: 23023155]
31. Ye J. Role of insulin in the pathogenesis of free fatty acid-induced insulin resistance in skeletal muscle. Endocr Metab Immune Disord Drug Targets. 2007; 7:65–74. [PubMed: 17346204]
32. Jin J, Zhang X, Lu Z, et al. Acid sphingomyelinase plays a key role in palmitic acid-amplified inflammatory signaling triggered by lipopolysaccharide at low concentrations in macrophages. Am J Physiol Endocrinol Metab. 2013; 305:E853–867. [PubMed: 23921144]
33. Uehata T, Akira S. mRNA degradation by the endoribonuclease Regnase-1/ZC3H12a/MCPIP-1. Biochim Biophys Acta. 2013; 1829:708–713. [PubMed: 23500036]
34. Schilling JD, Machkovech HM, He L, et al. Palmitate and lipopolysaccharide trigger synergistic ceramide production in primary macrophages. J Biol Chem. 2013; 288:2923–2932. [PubMed: 23250746]
35. Barsacchi R, Perrotta C, Bulotta S, et al. Activation of endothelial nitric-oxide synthase by tumor necrosis factor-alpha: a novel pathway involving sequential activation of neutral sphingomyelinase, phosphatidylinositol–3′ kinase, and Akt. Mol Pharmacol. 2003; 63:886–895. [PubMed: 12644590]
36. Yang Y, Yin J, Baumgartner W, et al. Platelet-activating factor reduces endothelial nitric oxide production: role of acid sphingomyelinase. Eur Respir J. 2010; 36:417–427. [PubMed: 19926744]
37. Gao D, Pararasa C, Dunston CR, et al. Palmitate promotes monocyte atherogenicity via *de novo* ceramide synthesis. Free Radic Biol Med. 2012; 53:796–806. [PubMed: 22640955]
38. Kelpe CL, Moore PC, Parazzoli SD, et al. Palmitate inhibition of insulin gene expression is mediated at the transcriptional level via ceramide synthesis. J Biol Chem. 2003; 278:30015–30021. [PubMed: 12771145]

Highlights

- We demonstrated how palmitic acid enhanced LPS in stimulation of IL-6 expression.
- GPR40, but not TLR4, was involved in palmitic acid-enhanced IL-6 expression.
- Palmitic acid augmented LPS-triggered MAPK and NFκB signaling activation.
- Sphingolipid metabolism was also involved in palmitic acid-enhanced IL-6 expression.

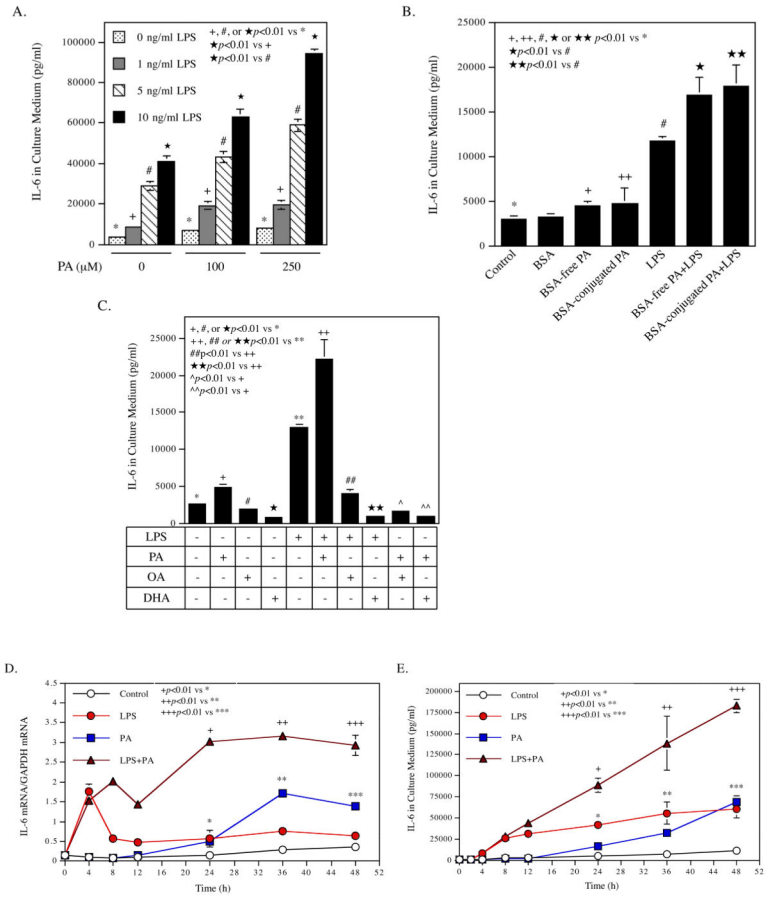

Figure 1.

The effect of LPS, PA or LPS plus PA on IL-6 expression in cardiac microvascular (MIC) endothelial cells (ECs). A. Concentration-dependent augmentation of LPS-stimulated IL-6 secretion by PA. MIC ECs were treated with different concentrations of LPS (0–10 ng/ml) in the absence or presence of 100 or 250 μM of PA for 24 h. After the treatment, IL-6 in culture medium was quantified using ELISA. B. The effect of BSA-free PA and BSA-conjugated PA on IL-6 secretion. MIC ECs were treated with 100 μM of either BSA-free PA or PA conjugated with low endotoxin BSA in the absence or presence of 5 ng/ml of LPS for 24 h and IL-6 in culture medium was then quantified. C. The effect of oleic acid (OA) or docosahexaenoic acid (DHA) on LPS- or PA-stimulated IL-6 secretion. MIC ECs were treated with 100 μM of PA, OA or DHA in the absence or presence of 5 ng/ml of LPS for 24 h and IL-6 in culture medium was then quantified. D and E. Time course of IL-6 mRNA expression (D) and IL-6 protein secretion (E) by MIC ECs treated with LPS, PA or LPS plus PA. MIC ECs were treated with 5 ng/ml of LPS, 100 μM of PA or LPS plus PA and the cells were harvested at 4, 8, 12, 24, 36, and 48 h. Total RNA was isolated from cells and IL-6 mRNA was quantified using real-time PCR. IL-6 mRNA was normalized to GAPDH mRNA. The culture medium from the above experiments was collected at each time point before the cell harvest and IL-6 protein in culture medium was quantified using ELISA.

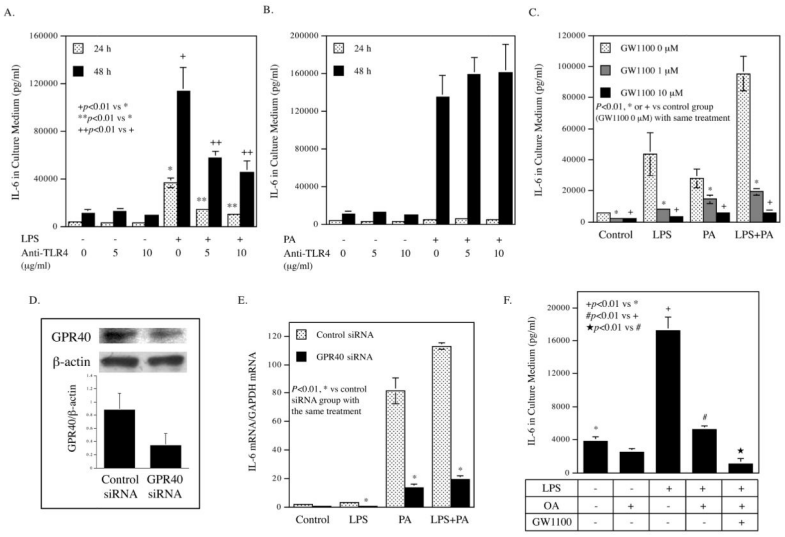

Figure 2.

LPS and PA upregulate IL-6 expression via different receptors. A and B. The effect of anti-toll-like receptor (TLR)4 antibodies on LPS- (A) or PA-stimulated (B) IL-6 secretion. MIC ECs were treated with 5 ng/ml of LPS or 100 μM of PA in the absence or presence of 5 or 10 μg/ml of anti-TLR4 antibodies for 24 or 48 h. After the treatment, IL-6 in culture medium was quantified. C. The effect of GPR40 antagonist GW1100 on IL-6 secretion stimulated by LPS, PA or LPS plus PA. MIC ECs were treated with 5 ng/ml of LPS, 100 μM of PA or LPS plus PA in the absence or presence of 1 or 10 μM of GW1100 for 24 h. After the treatment, IL-6 in culture medium was quantified. D. GPR40 protein expression in MIC ECs transfected with control siRNA or GPR40 siRNA. MIC ECs were transfected with 10 nM of control or GPR40 siRNA for 24 h and membrane protein was isolated for immunoblotting of GPR40. A representative immunoblotting of GPR40 was shown. The bands for GPR40 and β-actin from two immuneblots were quantified by densitometric analysis and the ratios of GPR40 vs β-actin were presented ($P<0.05$, control siRNA vs GPR40 siRNA). E. The effect of GPR40 siRNA on IL-6 expression stimulated by LPS, PA or LPS plus PA. MIC ECs were transfected with control siRNA or GPR40 siRNA for 24 h as described above and then treated with 5 ng/ml of LPS, 100 μM of PA or LPS plus PA for another 24 h. After the treatments, IL-6 mRNA was quantified using real-time PCR. The data are mean ± SD of a representative experiment from three experiments. F. The effect of GPR40 antagonist GW1100 on the inhibition by OA of IL-6 secretion stimulated by LPS. MIC ECs were treated with 5 ng/ml of LPS and/or 100 μM of OA in the absence or presence of 10 μM of GW1100 for 24 h. After the treatment, IL-6 in culture medium was quantified.

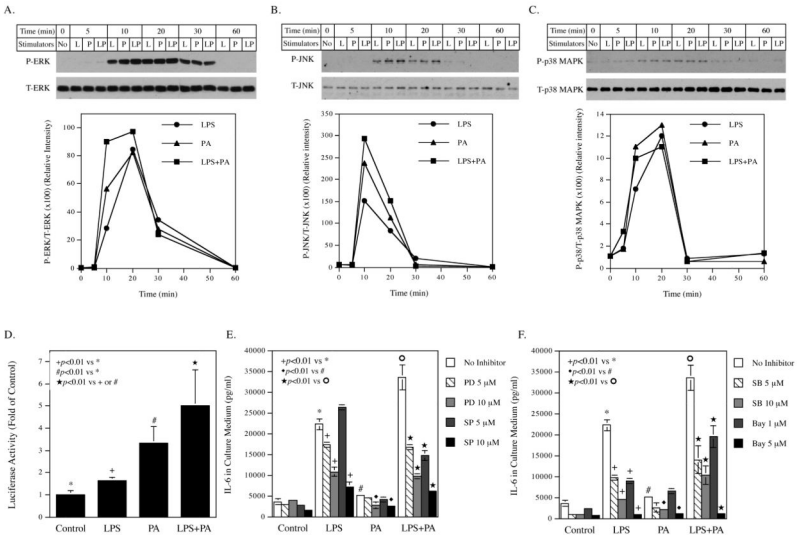

Figure 3.

The involvement of MAPK and NFκB signaling pathways in IL-6 secretion stimulated by LPS, PA or LPS plus PA. A-C. Activation of ERK (A), JNK (B) and p38 MAPK (C) by LPS, PA or LPS plus PA. MIC ECs were treated with 5 ng/ml of LPS [L], 100 μM of PA [P] or LPS plus PA [LP] for 5, 10, 20, 30 and 60 min. At each time point, cells were harvested for immunoblotting of phosphorylated and total ERK, JNK and p38 MAPK. The intensity of phosphorylated ERK, JNK and p38 MAPK was quantified and normalized to that of total ERK, JNK and p38 MAPK, respectively. D. The effect of LPS, PA or LPS plus PA on NFκB activity. MIC ECs were transfected with NFκB promoter-containing luciferase reporter vectors for 8 h and then treated with 5 ng/ml of LPS, 100 μM of PA or LPS plus PA for 24 h. After the treatment, cells were harvested for luciferase activity assays. E and F. Inhibition by pharmacological inhibitors of IL-6 secretion stimulated by LPS, PA or LPS plus PA. MIC ECs were treated with 5 ng/ml of LPS, 100 μM of PA or LPS plus PA in the absence or presence of 5 or 10 μM of PD98059 (PD), inhibitor for ERK pathway, 5 or 10 μM of SP600126 (SP), inhibitor for JNK pathway, 5 or 10 μM of SB203580 (SB), inhibitor for p38 MAPK pathway, or 1 or 5 μM of Bay11-7082 (Bay), inhibitor for NFκB pathway, for 24 h. After the treatment, IL-6 in culture medium was quantified.

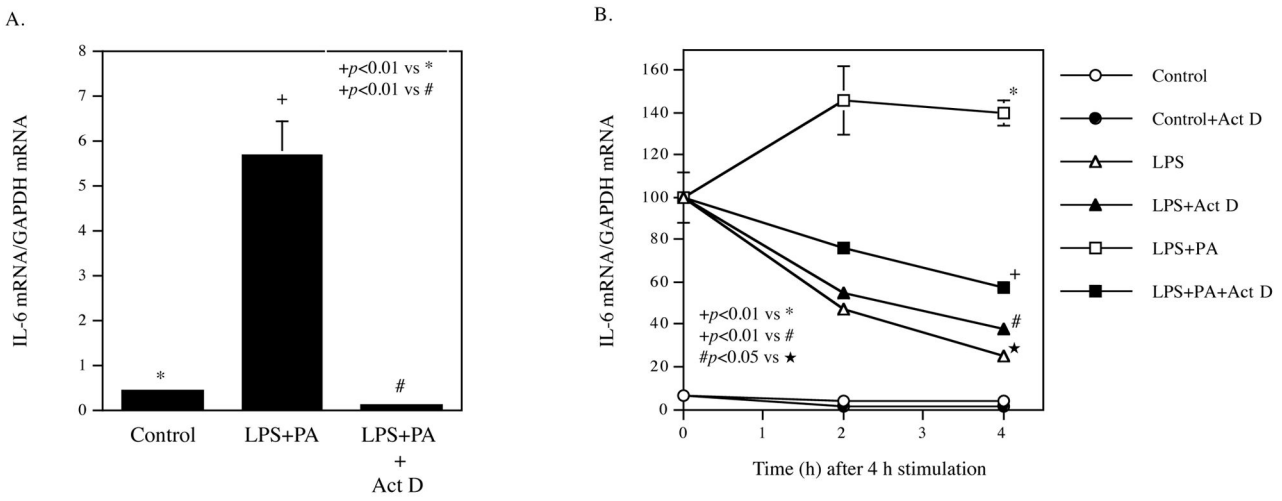

Figure 4.

Transcriptional and post-transcriptional regulation of IL-6 expression by LPS plus PA. A. Transcriptional activation of IL-6 expression by LPS plus PA. MIC ECs were treated with 5 ng/ml of LPS plus 100 μM of PA in the absence or presence of 5 μM of actinomycin D (Act D) for 6 h. After the treatment, cellular IL-6 mRNA was quantified. B. The effect of LPS or LPS plus PA on IL-6 mRNA stability. MIC ECs were treated without or with 5 ng/ml of LPS or 5 ng/ml of LPS plus 100 μM of PA for 4 h in the absence of Act D to induce IL-6 mRNA expression. After 4-h stimulation, Act D at 5 μM was added to part of the cells and the incubation was continued for the next 4 h. The cells were harvested at 0 h (right before adding Act D to cells), 2 h and 4 h after adding Act D, and IL-6 mRNA was quantified. The amount of IL-6 mRNA at 0 h was considered as 100%. IL-6 mRNA was normalized to GAPDH mRNA.

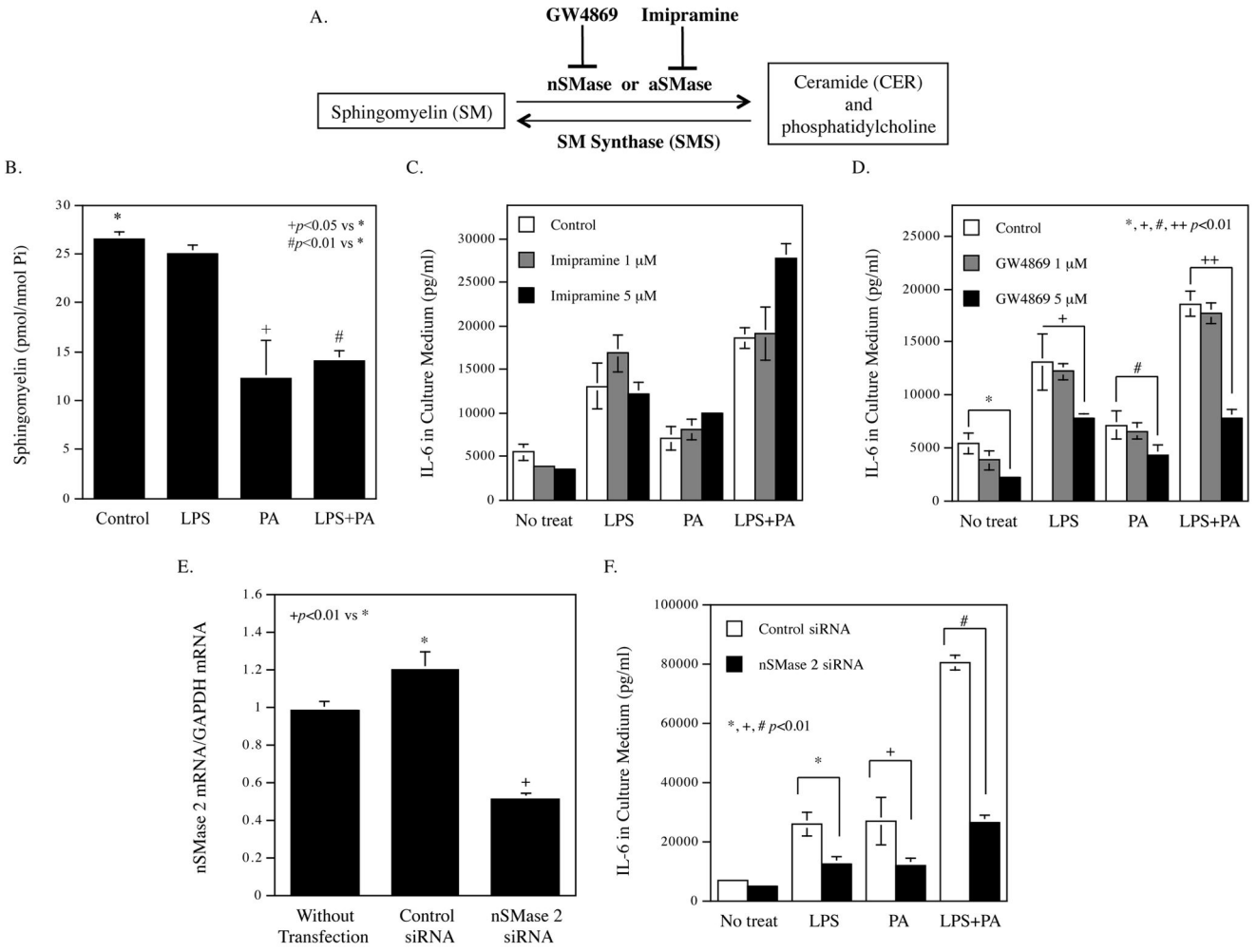

Figure 5.

The involvement of neutral sphingomyelinase (nSMase)-mediated sphingomyelin (SM) hydrolysis in IL-6 expression stimulated by LPS, PA or LPS plus PA. A. The SM metabolic pathway. B. The effect of LPS, PA or LPS plus PA on cellular SM level. MIC ECs were treated with 5 ng/ml of LPS, 100 μM of PA or LPS plus PA for 24 h and lipidomic analysis was conducted to quantify the cellular SM levels. C and D. The effect of imipramine (C) or GW4869 (D) on IL-6 expression stimulated by LPS, PA or LPS plus PA. MIC ECs were treated with 5 ng/ml of LPS, 100 μM of PA or LPS plus PA in the absence or presence of 1 or 5 μM of imipramine or GW4869 for 24 h. After the treatment, IL-6 in culture medium was quantified. E and F. The effect of nSMase 2 siRNA on IL-6 expression stimulated by LPS, PA or LPS plus PA. MIC ECs were transfected with 10 nM of control siRNA or nSMase2 siRNA for 24 h and nSMase 2 mRNA in untransfected cells or transfected cells was quantified (E). The transfected cells were treated with 5 ng/ml of LPS, 100 μM of PA or LPS plus PA for another 24 h and IL-6 in culture medium was quantified using ELISA (F).

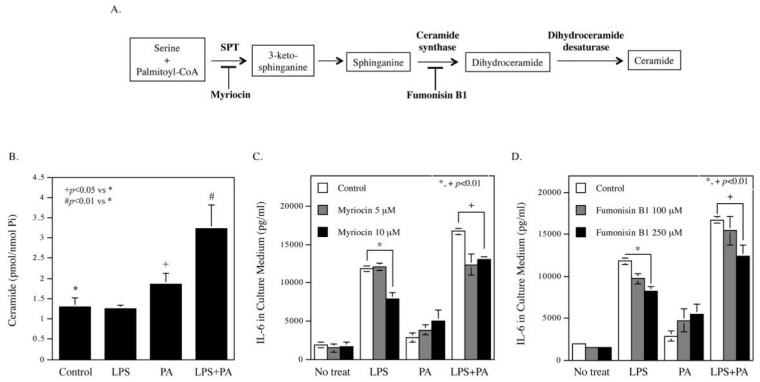

Figure 6.

The involvement of the *de novo* synthesis for ceramide (CER) in IL-6 expression in cardiac MIC ECs stimulated by LPS, PA or LPS plus PA. A. The metabolic pathway for *de novo* synthesis of CER. B. The effect of LPS, PA or LPS plus PA on cellular CER level. MIC ECs were treated with 5 ng/ml of LPS, 100 μM of PA or LPS plus PA for 24 h and lipidomic analysis was conducted to quantify the cellular CER levels. C and D. The involvement of the *de novo* synthesis of CER in IL-6 expression stimulated by LPS, PA or LPS plus PA. MIC ECs were treated with 5 ng/ml of LPS, 100 μM of PA or LPS plus PA in the absence or presence of 5 or 10 μM of myriocin (C) or 100 or 250 μM of fumonisin B1 (D) for 24 h. After the treatment, IL-6 in culture medium was quantified.

Table 1

Comparison of Stimulatory Effects of LPS and PA on Gene Expression

Genes	ΔCt between control and LPS	ΔCt between control and PA	Fold increase by LPS after 4 h stimulation	Fold increase by PA after 36 h stimulation
CCL2	2.46	< 1.00	6	< 2
CSF2	5.77	3.90	55	15
CSF3	6.95	5.48	124	45
CXCL10	1.82	< 1.00	4	< 2
FOS	< 1.00	2.00	< 2	4
HSPA1A	< 1.00	2.96	< 2	8
IFNG	< 1.00	1.11	< 2	2
IL-1A	2.66	2.77	6	7
IL-1B	3.96	4.03	16	16
IL-6	4.17	2.50	18	6
IL-8	3.05	2.22	8	5
IRAK2	2.23	0.94	5	2
IRF1	3.39	1.79	11	3
MAP3K1	1.08	< 1.00	2	< 2
NFKB2	1.47	1.07	3	2
NFKBIA	2.40	1.05	5	2
PTGS2 (COX-2)	1.96	2.06	4	4
REL	1.21	< 1.00	2	< 2
RIPK2	2.08	< 1.00	4	< 2
TNF alpha	3.22	1.90	9	4

Human cardiac MIC ECs were treated with 5 ng/ml of LPS for 4 h or 100 μM of PA for 36 h to achieve maximal stimulation by LPS or PA on gene expression. RNA was isolated from duplicate samples, combined and subjected to PCR array as described in the Methods.

Full names for the abbreviations: CCL2, chemokine C-C motif ligand 2, MCP-1; CSF2, colony stimulating factor 2; HSPA1A, heat shock 70kDa protein 1A; IFNG, interferon gamma; CXCL10, chemokine C-X-C motif ligand 10; IRAK2, interleukin-1 receptor-associated kinase 2; IRF1, interferon regulatory factor 1; MAP3K1, mitogen-activated protein kinase kinase kinase 1; NFKB2, nuclear factor of kappa light polypeptide gene enhancer in B-cells 2 (p49/p100); NFKBIA, nuclear factor of kappa light polypeptide gene enhancer in B-cells inhibitor, alpha; PTGS2, prostaglandin-endoperoxide synthase 2; REL, V-rel reticuloendotheliosis viral oncogene homolog; RIPK2, receptor-interacting serine-threonine kinase 2.

Table 2

The Cooperative Stimulation of Gene Expression by LPS and PA Treatment for 36 h

Genes	*Ct*				*ΔCt*			Fold increase by LPS	Fold increase by PA	Fold increase by LPS + PA
	Control	LPS	PA	LPS + PA	LPS − control	PA − control	(LPS + PA) − control			
CLEC4E	32.82	31.41	32.17	31.35	1.40	0.64	1.47	3	2	3
CSF2	29.68	27.86	25.78	25.22	1.82	3.90	4.46	4	15	22
CSF3	28.05	24.53	22.57	21.24	3.52	5.48	6.81	11	45	112
FOS	32.91	32.68	30.91	29.68	0.23	2.00	3.23	1	4	9
HSPA1A	28.90	28.24	25.94	25.66	0.67	2.96	3.24	2	8	9
IFNG	33.58	33.59	32.47	33.98	−0.01	1.11	−0.41	1	2	1
IL1A	28.27	28.13	25.50	25.53	0.14	2.77	2.74	1	7	7
IL1B	30.23	28.97	26.19	25.30	1.25	4.03	4.93	2	16	30
IL6	25.21	23.75	22.71	22.03	1.46	2.50	3.18	3	6	9
IL8	21.58	20.37	19.36	19.39	1.21	2.22	2.19	2	5	5
IRAK2	28.64	28.49	27.70	27.50	0.15	0.94	1.14	1	2	2
IRF1	29.16	28.67	27.37	27.61	0.49	1.79	1.56	1	3	3
NFKB2	28.12	27.83	27.05	27.76	0.28	1.07	0.36	1	2	1
NFKBIA	24.17	23.73	23.12	23.41	0.44	1.05	0.75	1	2	2
PTGS2	29.55	28.30	27.49	26.31	1.26	2.06	3.25	2	4	10
TLR2	31.32	31.86	30.40	29.54	−0.54	0.91	1.77	1	2	3
TNF	31.17	30.70	29.27	30.30	0.47	1.90	0.87	1	4	2

Human cardiac MIC ECs were treated with 5 ng/ml of LPS, 100 μM of PA or LPS plus PA for 36 h. RNA was isolated from duplicate samples, combined and subjected to PCR array as described in the Methods. Bold numbers indicate the cooperative effects by LPS and PA.

Full names for the abbreviations: CLEC4E, C-type lectin domain family 4, member E; CSF2, colony stimulating factor 2; HSPA1A, heat shock 70kDa protein 1A; IFNG, interferon gamma; IRAK2, interleukin-1 receptor-associated kinase 2; IRF1, interferon regulatory factor 1; NFKB2, nuclear factor of kappa light polypeptide gene enhancer in B-cells 2 (p49/p100); NFKBIA, nuclear factor of kappa light polypeptide gene enhancer in B-cells inhibitor, alpha; PTGS2, prostaglandin-endoperoxide synthase 2; REL, V-rel reticuloendotheliosis viral oncogene homolog (avian); RIPK2, receptor-interacting serine-threonine kinase 2.

Table 3

The Effect of GW4869 on SM Content in Response to LPS, PA and LPS plus PA

	C14- SM	C16-SM	C18-SM	C20-SM	C22-SM	C22:1-SM	C24-SM	C24:1-SM	Total SM	% of Control
Control	**0.72**	**9.22**	**0.36**	**0.11**	**0.87**	**0.59**	**4.22**	**9.71**	**25.80**	**100**
Control + GW4869	0.83	10.38	0.42	0.09	0.86	0.48	3.93	7.96	24.94	97
LPS	**0.78**	**9.71**	**0.45**	**0.10**	**0.86**	**0.53**	**4.08**	**8.49**	**25.01**	**97**
LPS +GW4869	1.03	10.60	0.53	0.11	0.97	0.57	4.57	9.31	27.69	107
PA	**0.33**	**4.86**	**0.48**	**0.10**	**0.70**	**0.47**	**2.84**	**5.20**	**14.98**	**58**
PA +GW4869	0.47	6.97	0.67	0.15	1.01	0.64	4.01	7.52	21.43	83
LPS+PA	**0.36**	**4.96**	**0.35**	**0.07**	**0.53**	**0.33**	**2.37**	**4.27**	**13.23**	**51**
LPS+PA +GW4869	0.48	7.11	0.53	0.11	0.81	0.50	2.96	5.68	18.19	71

Human cardiac MIC ECs were treated with 5 ng/ml of LPS, 100 μM of PA or LPS plus PA in the absence or presence of 5 μM of GW4869 for 24 h. The cells were then harvested for lipidomics analysis as described in Methods. The data presented in this Table is from one of two experiments. Unit: pmol/nmol Pi.

Table 4

The Effect of Myriocin on CER Content in Response to LPS, PA and LPS plus PA

	C14-Cer	C16-Cer	C18-Cer	C20-Cer	C22-Cer	C22:1-Cer	C24-Cer	C24:1-Cer	dhC16-Cer	Total Cer	% of Control
Control	**0.07**	**0.15**	**0.02**	**0.02**	**0.07**	**0.05**	**0.36**	**0.64**	**0.03**	**1.46**	**100**
Control +myriocin	0.04	0.05	0.01	0.01	0.03	0.02	0.08	0.22	0.02	0.47	32
LPS	**0.08**	**0.09**	**0.02**	**0.01**	**0.07**	**0.05**	**0.30**	**0.59**	**0.03**	**1.28**	**87**
LPS +myriocin	0.05	0.04	0.01	0.01	0.04	0.02	0.09	0.22	0.02	0.51	35
PA	**0.14**	**0.22**	**0.09**	**0.06**	**0.31**	**0.13**	**0.53**	**0.69**	**0.20**	**2.26**	**155**
PA +myriocin	0.11	0.18	0.08	0.06	0.31	0.09	0.91	0.59	0.08	2.36	161
LPS+PA	**0.16**	**0.35**	**0.12**	**0.07**	**0.39**	**0.16**	**0.63**	**0.82**	**0.35**	**2.79**	**191**
LPS+PA +myriocin	0.15	0.22	0.04	0.02	0.15	0.09	0.68	0.76	0.04	2.19	150

Human cardiac MIC ECs were treated with 5 ng/ml of LPS, 100 μM of PA or LPS plus PA in the absence or presence of 10 mM of myriocin for 24 h. The cells were then harvested for lipidomics analysis as described in Methods. The data presented in this Table is from one of two experiments. Unit: pmol/nmol Pi.